Stable isotope chronology and climate signal calibration in neotropical montane cloud forest trees

K. J. Anchukaitis,[1,2,3] M. N. Evans,[1,2] N. T. Wheelwright,[4] and D. P. Schrag[5]

[1] Tropical montane cloud forests are ecosystems intrinsically linked to a narrow range of geographic and meteorological conditions, making them potentially sensitive to small changes in precipitation or temperature. We investigate the potential application of stable isotope analysis to cloud forest dendroclimatology at Monteverde in Costa Rica in order to be able to extract both chronological and paleoclimate information from trees without annual growth rings. High-resolution $\delta^{18}O$ measurements are used to identify regular cycles in wood of up to 9‰, which are associated with seasonal changes in precipitation and moisture sources. The calculated annual growth rates derived from the isotope time series match those observed from long-term basal growth measurements. Interannual variability in the oxygen isotope ratio of lower forest trees is primarily related to interannual changes in wet season precipitation. Forward modeling independently supports our detection of both annual chronology and a climate signal. The confirmation of annual chronology and sensitivity to interannual climate anomalies suggests that tropical cloud forest dendroclimatology can be used to investigate local and regional hydroclimatic variability and change.

1. Introduction

[2] In the absence of long instrumental records, scientists investigating the causes and consequences of climate variability and change depend on proxy records, which can be used to reconstruct past ocean–atmosphere conditions. In temperate latitudes, extensive networks of tree ring width and density time series ("chronologies") provide a high-resolution proxy record of past climate state and variability. Relatively few such chronologies, however, have been developed in tropical regions. Despite some notable exceptions [cf. *Worbes*, 2002; *Brienen and Zuidema*, 2005; *D'Arrigo et al.*, 2006; *Therrell et al.*, 2006; *Buckley et al.*, 2007], tropical trees often fail to develop reliable annual rings whose variability consistently reflects the influence of climate and can be used to reconstruct past temperatures or precipitation. Even when they appear to form annual increment bands, patterns of ring width variability may be incoherent between individual trees, making both chronology development and climate signal detection difficult

[*Worbes and Junk*, 1989; *February and Stock*, 1998; *Dünisch et al.*, 2002; *Robertson et al.*, 2004; *Bauch et al.*, 2006]. As a consequence, high-resolution, long terrestrial proxy climate records from the tropics remain sparse compared with temperate regions.

[3] Tropical montane cloud forests cover as much as 50 million hectares worldwide [*Stadtmüller*, 1987; *Hamilton et al.*, 1995], about half of which is found in Latin America [*Brown and Kappelle*, 2001]. These forests have high rates of endemism and are important in regional hydrology, because they intercept and capture cloud moisture and nutrients, increasing available water and influencing biogeochemistry within catchments and in areas downstream [*Bruijnzeel*, 1991, 2004; *van Dijk and Bruijnzeel*, 2001]. Tropical cloud forests are ecosystems found within a relatively narrow set of both geographic and meteorological conditions, and as a consequence, they are particularly sensitive to climate change [*Loope and Giambelluca*, 1998; *Foster*, 2001; *Bush*, 2002].

[4] Rising tropical air and sea surface temperature associated with anthropogenic global climate change may be fundamentally altering the suite of environmental conditions that create and maintain unique cloud forest ecosystems. At Monteverde, in the mountains of Costa Rica, the extinction of the endemic Golden Toad (*Bufo periglenes*) in 1987 and subsequent additional reptile and anuran declines have been linked to apparent decreases in cloud cover and moisture availability and related to changing temperatures [*Pounds et al.*, 1999]. Indeed, temperature trends in montane regions throughout the tropics have been linked to widespread disease-linked species extinction and alterations to cloud

[1]Laboratory of Tree-Ring Research, University of Arizona, Tucson, Arizona, USA.
[2]Department of Geosciences, University of Arizona, Tucson, Arizona, USA.
[3]Now at Lamont-Doherty Earth Observatory, Columbia University, Palisades, New York, USA.
[4]Department of Biology, Bowdoin College, Brunswick, Maine, USA.
[5]Department of Earth and Planetary Sciences, Harvard University, Cambridge, Massachusetts, USA.

forest biogeography [*Pounds et al.*, 2006]. A rise in tropical air temperatures above 1000 meters has been observed since 1970 [*Diaz and Graham*, 1996]. Climate change appears to be exposing plant and animal communities to increased environmental stress, which may exacerbate other proximal threats, including disease and habitat destruction [*Root et al.*, 2003; *Pounds et al.*, 2006].

[5] Limited long-term instrumental climate records from the tropics, and in particular tropical montane regions [*Bradley et al.*, 2006], impede efforts to better understand both global climate variability and its influence on local hydroclimatology and ecology. Without a historical baseline and the context provided by long-term climate records, it is difficult to attribute the observed changes in climate and ecological systems at Monteverde and other tropical mountain forests to anthropogenic climate forcing [*Still et al.*, 1999; *Pounds et al.*, 2006], mesoscale influences including land clearance [*Lawton et al.*, 2001; *Nair et al.*, 2003], or natural variability in tropical and extratropical climate. Limited observational data and the lack of high resolution proxies from these ecosystems also restrict any opportunity to validate GCM predictions for future change [*Foster*, 2001]. Both observed and potential future changes, and their hypothesized ecological consequences, need to be placed in the context of low-frequency (decadal to centennial) climate variability and trends over the recent past. Climate reconstructions from tropical montane cloud forests would provide the necessary context for the interpretation of the limited instrumental climate record, and allow the identification of variability or trends that are outside of the range of natural variability.

[6] We hypothesize that the unique hydroclimatic conditions associated with cloud forests creates an annual climate signal in the oxygen isotope ratio (δ^{18}O) in tree xylem cellulose that can be used to develop a proxy record of climate variability from tropical montane regions. High-resolution oxygen isotope measurements can be used for both chronological control and climatic interpretation and reconstruction. Our study focuses on the Monteverde Cloud Forest in Costa Rica where environmental and meteorological data [*Nadkarni and Wheelwright*, 2000], available over the last 20 years, provides the data necessary to validate this hypothesis. Our ultimate goal is to develop the necessary basis for proxy reconstructions of interannual tropical climate variability using stable oxygen isotope series from cloud forest trees without annual rings.

2. A Stable Isotope Approach to Cloud Forest Dendroclimatology

[7] Tropical montane cloud forests are ecosystems characterized by frequent or persistent orographic cloud immersion [*Bruijnzeel and Veneklaas*, 1998]. During the dry season, water stripped from the cloud bank by vegetation provides sufficient soil moisture such that trees may experience no effective water deficit [*Bruijnzeel and Proctor*, 1995; *Kapos and Tanner*, 1985; *Holder*, 2004]. Precipitation, which provides the bulk of available water during the rainy season, and cloud water, which is the primary moisture source during the dry season, are isotopically distinct [*Ingraham*, 1998]. Phase transitions between liquid and vapor result in fractionation effects, which create isotopic

differences between these two water sources. Condensation of clouds by orographic uplift results in liquid water which has relatively heavy δ^{18}O values as compared with rainfall, which has a lower δ^{18}O value due to progressive Rayleigh distillation [*Ingraham*, 1998]. Similarly, the limited amount of rainfall received during the dry season has a relatively heavy δ^{18}O signature. This is related primarily to the "amount effect", where the δ^{18}O of precipitation is negatively correlated to the quantity, and is one of the primary causes of intra-annual patterns in the isotopic composition of rainfall throughout the tropics [*Gat*, 1996]. The amount effect is evident in the stable isotopic composition of Costa Rican surface waters [*Lachniet and Patterson*, 2002].

[8] Data from both Monteverde [*Feild and Dawson*, 1998] and other fog-dependent environments [*Ingraham and Matthews*, 1990, 1995; *Dawson*, 1998; *Fischer and Still*, 2007; *Scholl et al.*, 2007] indicate that differences of at least 4‰ to 6‰ may exist between cloud water and rainfall. *Rhodes et al.* [2006] and *Guswa et al.* [2007] also report differences between dry (boreal winter) and wet (boreal summer) season volume-weighted precipitation and throughfall δ^{18}O from Monteverde as great as 9‰. The waters available to plants in cloud forest ecosystems are therefore distinctly different between seasons. *Feild and Dawson* [1998] confirmed that the xylem water of canopy trees at Monteverde had the isotopic signature of rainfall during the wet season. Cloud water should be one of the primary water sources available to trees during the dry season [cf. *Dawson*, 1998]. However, at Monteverde dry season precipitation and cloud water have overlapping δ^{18}O signatures [*Schmid*, 2004; *Scholl et al.*, 2007], so that trees may draw from a mixed moisture source but with an overall enriched oxygen isotope composition compared with that of wet season rainfall [*Guswa et al.*, 2007].

[9] These seasonal changes in the isotopic composition of the primary water sources for trees in cloud forests should produce a seasonal cycle in the oxygen isotope ratio of cellulose in the secondary radial growth of these trees. Fine-scale analysis of isotope ratios of cellulose along the growth radius of a tree's main trunk will yield a time series of water use by the trees. The seasonal cycle can be used to identify the growth increment from an individual year (with 1 cycle = 1 calendar year), even in the absence of visible annual banding [*Evans and Schrag*, 2004]. Significant departures from the regular isotope cycle should result from local hydroclimatic alterations, including precipitation anomalies and changes in cloudiness, moisture advection, relative humidity, and temperature (Figure 1).

[10] The relationship between the local hydroclimatology of tropical montane cloud forests and the resulting δ^{18}O value of cellulose in trees can be understood using the mechanistic model developed by *Roden et al.* [2000]:

$$\delta^{18}O_{cellulose} = f_o \cdot (\delta^{18}O_{wx} + \epsilon_o) + (1 - f_o) \cdot (\delta^{18}O_{wl} + \epsilon_o) \quad (1)$$

where $\delta^{18}O_{cellulose}$ is the oxygen isotope ratio of tree ring cellulose, $\delta^{18}O_{wx}$ is the oxygen isotope ratio of unenriched xylem water in the stem, $\delta^{18}O_{wl}$ is the oxygen isotope ratio of leaf water at the sites of photosynthesis, f_o is the fraction of oxygen in stem water that does not exchange with the enriched sucrose that results from transpiration in the leaf,
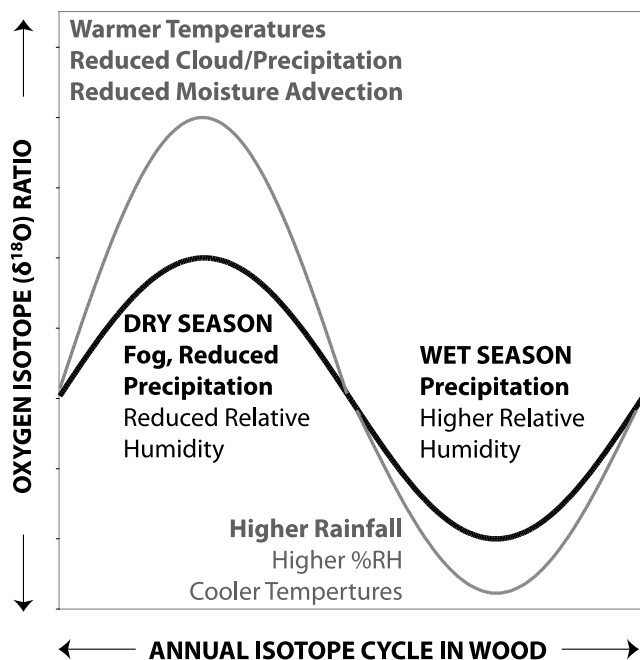
Figure 1. Conceptual model of climatic controls on the annual and interannual patterns of stable oxygen isotope ratios in the of cloud forest tree radial growth. The annual cycle is generated primarily by the seasonal change in the $\delta^{18}O$ of rainfall, the use of cloud water by trees in the dry season, and the isotopic enrichment of source water by evapotranspiration during the dry season. Interannual variability in annual maximum values is expected to be related to temperature, relative humidity, cloudiness, and moisture advection during the dry season. Anomalies in the annual minima are likely related primarily to wet season precipitation amounts.

and ϵ_o is the fractionation that results from the synthesis of cellulose. This model shows that α-cellulose $\delta^{18}O$ is influenced primarily by the $\delta^{18}O$ of the source water taken up by the plant, and by the amount of isotopic enrichment of that water that subsequently occurs in the leaf, and whose signature is inherited by the sucrose used in the eventual biosynthesis of cellulose. As detailed above, source water differences in cloud forests will be a function of the seasonal regimes of rainfall and cloud water. Lower relative humidity levels during the peak of the dry season should result in higher evapotranspiration rates and enrichment of the $\delta^{18}O$ value of leaf water and the resultant cellulose.

[11] *Barbour et al.* [2004] modified the model of *Roden et al.* [2000] to include the potential influence of the Peclet effect, a diffusion of isotopically enriched water away from the sites of transpiration in the leaves back into the unenriched source water, which results in lower $\delta^{18}O$ value for bulk leaf water than would be predicted from a simple calculation based on evapotranspiration in the leaf [*Barbour et al.*, 2000]:

$$\Delta_c = \Delta_l(1 - p_x p_{ex}) \qquad (2)$$

For our purposes, Δ_c is the enrichment of the cellulose $\delta^{18}O$ above that of the original source water, and Δ_l reflects the enrichment of the source water signal in the leaf at the sites of photosynthesis, as a function of leaf temperature, the vapor pressure difference within the leaf, the $\delta^{18}O$ of atmospheric water vapor, the fractionation associated with the liquid–vapor phase change, and the Peclet effect:

$$\Delta_l = \left\{ (1 + \epsilon^*) \left[1 + \epsilon_k + (\Delta_{wva} - \epsilon_k)\frac{e_s}{e_i} \right] - 1 \right\} \left(\frac{1 - e^{-\varphi}}{\varphi} \right) \qquad (3)$$

where ϵ^* and ϵ_k are the temperature-dependent equilibrium and kinetic liquid–vapor fractionation factors, Δ_{wva} is the isotopic composition of the atmospheric water vapor, and e_s and e_i are the leaf surface and interstitial water vapor pressure. The Peclet number φ is calculated from the effective evaporative pathway length (L), the evaporation rate (E), the molar density of water, and the diffusivity of $H_2^{18}O$ in water [*Barbour et al.*, 2004].

[12] p_{ex} is the proportion of oxygen atoms exchanged during the formation of cellulose from sucrose, equivalent to f_0 from equation (1). p_x is the proportion of unenriched water at the site of cellulose formation. In large trees, cellulose formation in the xylem, p_x should approach 1, as the site of cellulose synthesis is sufficiently distal from the diffusion of enriched leaf water into unaltered source water that it is primarily those waters that provide the exchangeable oxygen during cellulose biosynthesis [*Barbour et al.*, 2002]. In this case, $p_x p_{ex}$ is equivalent to f_0 from equation (1) and represents the mixing between enriched $\delta^{18}O$ signatures from the leaf and $\delta^{18}O$ from the original source water. The derivation, parameterization, and interpretation of these modeled relationships between climate and wood cellulose are described in detail by *Barbour et al.* [2004] and *Evans* [2007].

[13] We hypothesize (Figure 1) that the isotopic difference between wet season precipitation and dry season rainfall and cloud water is sufficient to generate annual isotope cycles in the xylem of cloud forest trees. We rely on the seasonal shift in primary water source to drive concomitant changes in cellulose, enabling identification of annual cycles and chronology development. Interannual variability should be manifested as enhancement or suppression of the amplitude of the mean annual isotope cycle through changes in precipitation, temperature, and relative humidity. Year-to-year differences in annual maximum values are expected to be related to temperature, relative humidity, cloudiness, and moisture advection during the dry season. Anomalies in the annual minima are likely related primarily to wet season precipitation amounts.

3. Methods and Materials

[14] We test our hypotheses using samples and data collected from the Monteverde Cloud Forest Reserve in Costa Rica. Long-term vegetation monitoring and daily climate records [*Pounds et al.*, 1999; *Clark et al.*, 2000; *Nadkarni and Wheelwright*, 2000; *Rhodes et al.*, 2006] from the Reserve are used to calibrate, model, and interpret the $\delta^{18}O$ content of tree cellulose, making the site an ideal location in which to establish if the necessary chronological control and climate signal exist. Establishing both of these
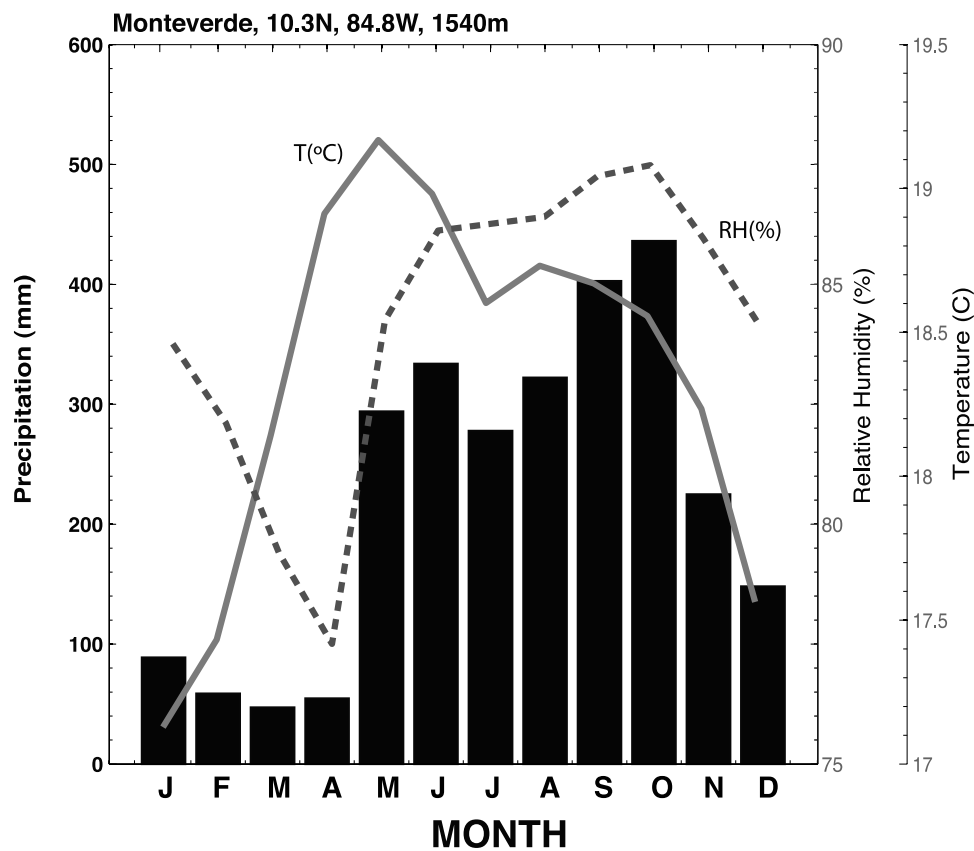
Figure 2. Patterns of mean annual temperature and precipitation for Monteverde from the Campbell weather station and derived relative humidity (1979–2000, 10.2°N, 85.35°W, 1540 m [*Pounds et al.*, 1999]).

is a necessary prerequisite for the development of robust climate reconstructions.

3.1. Site Description

[15] The Monteverde Cloud Forest (10.2°N, 85.35°W, 1500 m) is draped over the Cordillera de Tilarán in northwestern Costa Rica. The cloud forest extends from ~1500 m on the Pacific slope upward to the continental divide, and down the windward Atlantic slope as low as 1300 m [*Haber*, 2000]. Below the cloud forest and downslope to 700 m elevation on the leeward Pacific slope the vegetation is predominantly evergreen tropical premontane wet forests with a distinct dry season. Between 1400 and 1500 m, the premontane forest transitions to lower montane wet forests with greater orographic cloud influence [*Haber*, 2000]. The cloud forest above 1500 m receives an average of 2500 mm of precipitation in a year and has a mean annual temperature of 18.5°C [Figure 2; *Pounds et al.*, 1999; *Clark et al.*, 2000]. These forests are characterized by the presence of tradewind-driven orographic clouds in the transitional (November through January) and dry (February through April) seasons. During the wet season (May through October), the precipitation regime is dominated by the position of the Intertropical Convergence Zone (ITCZ) and characterized by strong convective rainfall and thunderstorms [*Clark et al.*, 2000; *Rhodes et al.*, 2006]. A midsummer "drought" (*veranillo*), common to the Pacific Coast of tropical Central America [*Magaña et al.*, 1999], is present

in July and August (Figure 2). The cloud forest receives the majority of its rainfall during the wet season, but the annual moisture regime has substantial and seasonally important inputs from orographic cloud water between November and April. Whereas the Atlantic slope is perpetually wet, the leeward slope depends on the northeasterly trade wind-driven moisture over the continental divide as a critical dry season water source. *Clark et al.* [1998] found that at Monteverde these moisture inputs accounted for perhaps 22% of the annual hydrological budget. However, estimates of the contribution from cloud water at an array of tropical montane cloud forest sites vary from <1% up to 74%. [*Bruijnzeel and Proctor*, 1995; *Bruijnzeel*, 2001]. Cloud water inputs are consistently more important during the dry season, accounting for up to 75% of total seasonal moisture inputs in some forests [*Bruijnzeel*, 2001].

3.2. Field and Laboratory Sampling

[16] We take advantage of two stands of monitored *Ocotea tenera* (Lauraceae) from experimental plots in the transitional zone between lower montane and cloud forest [*Wheelwright and Logan*, 2004] in order to calibrate and confirm our hypothesized age model and precisely evaluate potential climate signals. *O. tenera* is a deciduous, dioecious understory tree which is endemic to Costa Rica [*Wheelwright and Bruneau*, 1992]. It is reproductively mature at 5 years, at which time it can have a diameter as small as 1.5 cm. The largest individuals may grow up to

30 cm diameter. Increment cores from *O. tenera* were collected in February 2004 from the Trostles (NWT-) and Hoges (NWH-) experimental plots. These plots were established in 1981 and 1984, respectively, and are situated in shaded secondary forest with emergent canopy trees [*Wheelwright and Logan*, 2004]. Three cores were obtained from the Trostles plot, with two collected from a single tree (NWT02A/B), and one from a separate individual (NWT01A). A fourth core was collected from the Hoges plot (NWH03A). This sampling approach was designed to evaluate the fidelity and consistency of the chronological and climatic signal both within and between trees, and among sites. Annual diameter measurements made at a height of 1 m with calipers in February or March are available for all three trees since 1988 [see *Wheelwright and Logan*, 2004].

[17] In addition, to the trees from the experimental plots, nine additional cores or entire cross-sectional discs were also opportunistically collected in and around the Monteverde Cloud Forest Reserve (1500–1660 m) from mature unmonitored canopy trees, many which had been felled in a December 2003 windstorm. This group included individuals from the genus *Quercus* (oaks) as well as from the cosmopolitan Sapotaceae and Lauraceae families. The forest trees were sampled along a rudimentary transect up the Pacific slope toward the continental divide. This strategy was intended to accomplish two complementary goals. First, it permits discovery of sites or species that have maximum sensitivity to both annual and interannual changes in climate. Second, the comparison of $\delta^{18}O$ values from both below and within the cloud bank should allow us to estimate the relative importance across the landscape of changes in precipitation, temperature, and relative humidity to the α-cellulose $\delta^{18}O$ of cloud forest trees.

3.3. Sample Preparation

[18] The cores were subsampled in the laboratory on a rotary microtome at 20 μm increments. Ten slices were then aggregated into a single sample for a sampling depth resolution of 200 μm. Our subsampling interval resulted in approximately 700 to 1500 μg of wood per sample, depending on wood density, structure, and moisture content. Radial subsections approximating the diameter of the cores (5 mm) were cut from the large full stem discs using a bandsaw prior to microtoming.

[19] Raw wood was then extracted to α-cellulose using the standard Brendel technique [*Brendel et al.*, 2000; *Anchukaitis et al.*, 2008] as modified for small samples [*Evans and Schrag*, 2004]. The Brendel procedure uses a hot 10:1 acetic/nitric acid delignification extraction that also removes most hemicelluloses and mobile resins, followed by progressive solvent washes and sample drying in distilled water, ethanol, and acetone [*Evans and Schrag*, 2004; *Anchukaitis et al.*, 2008]. Following extraction, samples were dried in a warm oven (50°C), and then overnight under vacuum. Use of the Brendel technique allows for single-day chemical preprocessing of samples and, most critically, permits the use of very small (<1 mg) samples with a sufficient final sample yield [*Evans and Schrag*, 2004] for replicate isotopic measurements. The Brendel technique results in α-cellulose that is not significantly different in

its isotopic composition compared with traditional methods [*Evans and Schrag*, 2004; *Anchukaitis et al.*, 2008].

3.4. Isotopic Analysis

[20] 100 to 150 μg of α-cellulose of each sample from the *O. tenera* cores were wrapped in silver capsules and converted to CO in a ThermoFinnigan Thermal Conversion/Elemental Analyzer (TC/EA) at 1450°C. The oxygen isotope composition of the CO gas was analyzed on a ThermoFinnigan Delta XL continuous flow mass spectrometer at Harvard University. Measurement precision for several hundred Baker α-cellulose standards was 0.45‰.

[21] For the analysis of pilot samples from canopy trees in the Monteverde Cloud Forest Preserve, 300 to 350 μg of α-cellulose were loaded in silver capsules and converted online to CO in a Costech High Temperature Generator/ Elemental Combustion System (HTG/ECS) system with a quartz outer reactor and molybdenum crucible packed with graphite [*Evans*, 2008]. Our HTG pyrolysis system at The University of Arizona is a 1 MHz radio frequency induction heater which quickly brings the molybdenum susceptor inside the reactor assembly to >1500°C, at which time the sample is introduced to the crucible and pyrolysed under a continuous flow of pure helium. Use of the HTG peripheral reduces laboratory consumables, simplifies reactor maintenance and replacement, and results in an efficient high-temperature conversion of the sample to CO [*Evans*, 2008]. Our study here is the first application of this technology to paleoenvironmental research using oxygen isotopes. The isotopic ratio of the CO gas was measured on a Thermo-Finnigan Delta + XP. Precision on several hundred Sigma Alpha Cellulose (SAC) solid standard material was 0.32‰. All $\delta^{18}O$ results from both instruments are reported with respect to the international Vienna Standard Mean Ocean Water (VSMOW).

3.5. Forward Modeling

[22] We use the *Barbour et al.* [2004] model (described above) of the environmental controls on the stable isotope composition of wood, as modified and adapted for time series prediction in tropical environments by *Evans* [2007], to simulate a theoretical monthly stable oxygen isotope time series based on local meteorological data. Synthetic isotope time series are then compared with our actual measured $\delta^{18}O$ chronology from *O. tenera* to independently test the age model and climate signal detection.

[23] The model takes as input monthly temperature, precipitation, and relative humidity data [*Evans*, 2007]. There are 14 parameters in the model (7 from the original *Barbour et al.* [2004] model, 7 from the extension of the model to time series simulation), which are described in detail by *Barbour et al.* [2004] and *Evans* [2007]. Many of these are only weakly constrained by observations, particularly for tropical species and environments. Therefore as in *Evans* [2007], we use a Monte Carlo procedure (1000 simulations) and randomized adjustments (up to 20%) of the default model parameters from *Barbour et al.* [2004] to estimate the sensitivity of the interannual patterns of variability to the selection of the parameter values.

[24] Following *Evans* [2007], we parameterized leaf temperature as a function of air temperature [*Linacre*, 1964]. Atmospheric water vapor $\delta^{18}O$ was calculated as a function
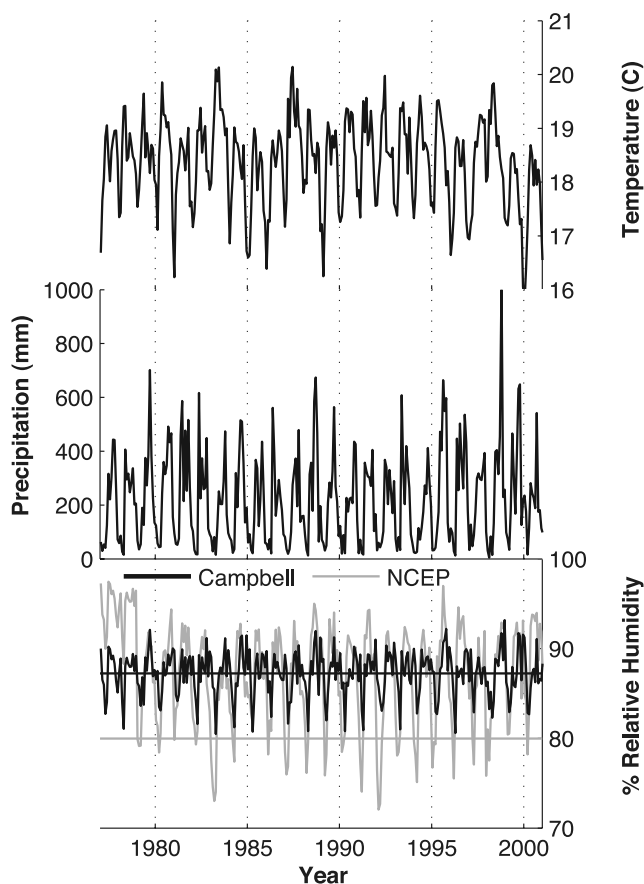
Figure 3. Meteorological data from Monteverde used as input for the forward model of tree α-cellulose δ^{18}O. (a) Temperature ($^\circ$C) and (b) precipitation from the Campbell meteorological station [*Pounds et al.*, 1999] and (c) relative humidity derived from the Campbell data and from the NCEP Reanalysis 2 [*Kanamitsu et al.*, 2002]. The NCEP relative humidity has been scaled to give it the same mean as that observed in *Rhodes et al.* [2006], but allowed to retain its variance. The horizonal lines of the same color show the original overall mean value. Sensitivity to the choice of relative humidity data is 0.20‰ per month per percent mean relative humidity.

of condensation temperature and the isotopic fractionation related to the vapor–liquid phase change [*Gonfiantini et al.*, 2001], although in practice a simpler Rayleigh model ($\delta^{18}O_{wva} = \delta^{18}O_{sw} - 8$) also gives nearly identical results. *Evans* [2007] derived stomatal conductance (G_s) as a function of vapor pressure deficit (D_s) calculated from monthly air and derived leaf temperature and observed relative humidity. This allows stomatal conductance (G_s), and therefore transpiration (E), to vary temporally in response to environmental conditions [*Jarvis and McNaughton*, 1986],

$$E = G_s D_s / P_{atm} \qquad (4)$$

where P_{atm} atm is monthly mean atmospheric pressure, which absent local observations is assumed constant. The δ^{18}O of water at the site of photosynthesis in the leaves is calculated as a change in source water δ^{18}O as a function of

kinetic and equilibrium diffusive fractionation, leaf temperature, water vapor δ^{18}O and the vapor pressure gradient between the leaf and atmosphere (equation (3)). Two additional parameters provide the coefficients for the model relating precipitation to δ^{18}O of meteoric waters (see below).

[25] Precipitation and temperature data are available from the Campbell ($\sim$1540 m) weather station [*Pounds et al.*, 1999] for the period 1977 to 2005, and from the Monteverde Institute [*Rhodes et al.*, 2006] from 2004 through 2006 (1420 m). We calculated the monthly source water δ^{18}O as a function of the observed relationship between rainfall amount and the δ^{18}O composition of rainfall (the amount effect) from *Rhodes et al.* [2006]. We regressed the δ^{18}O on rainfall amounts for those data with aggregate collection periods of two weeks to two months. Single-storm events and shorter collection periods showed a higher variability which likely reflected the time of sampling and the trajectory and history of individual weather systems, while longer periods excessively smoothed monthly differences related to the timing and onset of precipitation seasonality. Three samples which were observed by *Rhodes et al.* [2006] to have algae growing on the collection container were excluded from the regression model. Source water δ^{18}O values were then calculated based on monthly total precipitation values from the Campbell data set:

$$\delta^{18}O_{sw}‰ = -0.0155 \times P(mm/month) - 1.2614 \qquad (5)$$

[26] The regression model accounts for 56% of the variance in the observed data set and is significant at $p < 0.01$ with 14 effective degrees of freedom.

[27] The *Rhodes et al.* [2006] data also includes relative humidity for July 2005 through the end of 2006. In order to develop modeled synthetic chronologies that spanned the full timescale of our oxygen isotope chronologies from the *O. tenera* experimental plots, we derived a relative humidity time series to use with the model by regressing the daily relative humidity measurement from *Rhodes et al.* [2006] on the maximum daily temperature and daily precipitation values for the same station. This model was then applied to create a daily relative humidity time series spanning the full length of the Campbell [*Pounds et al.*, 1999] daily temperature and precipitation record:

$$RH\% = (-1.0191 \times Tmax(C)) + (0.2459 \times P(mm)) \\ - 105.1180 \qquad (6)$$

[28] The regression model accounted for 43% of the variance, and was significant at $p < 0.01$. Relative humidity values were then adjusted so that the long-term seasonal mean and variance matched those from the observations by *Rhodes et al.* [2006]. This relationship necessarily reflects relative humidity condition in the lower cloud forest transition zone, where both the experimental plots and the *Rhodes et al.* [2006] meteorological station are found. Daily values for temperatures, precipitation, and relative humidity were then combined to form monthly means and total precipitation for model input (Figure 3). We also extracted a time series of monthly relative humidity from the NCEP Reanalysis II gridded data [*Kanamitsu et al.*, 2002] for the
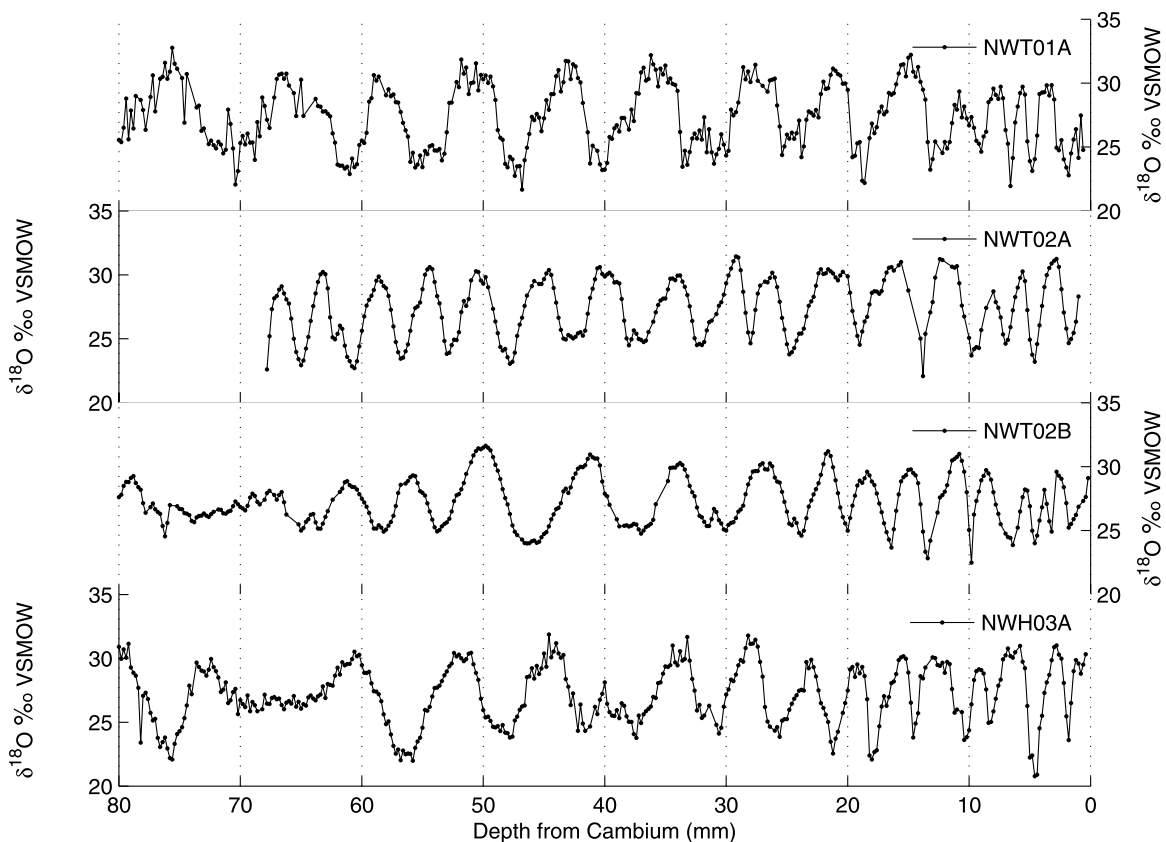
Figure 4. Isotope ratios as a function of sampling depth for the four *O. tenera* from the Trostles and Hoges plots. Individual samples are indicated by dots. In NWT02B and NWH03A, samples across or close to the pith can be seen in the $\delta^{18}O$ plateau near the center of the tree.

latitude, longitude, and atmospheric pressure level (850 mb) that most closely corresponds to the Monteverde Cloud Forest, in order to test the sensitivity of our results to the choice of available relative humidity data.

[29] *Evans* [2007] used the forward model to reconstruct the patterns of interannual variability in $\delta^{18}O$ cycles in tropical trees from La Selva Biological Station in Costa Rica. In those simulations, the mean and variance of the simulation were adjusted to that of the observed $\delta^{18}O$ time series. Here however, we use a simple single-component soil mixing model in place of the variance adjustment to capture the influence of the temporal smoothing of individual monthly water $\delta^{18}O$ as a result of soil water residence times.

4. Results

4.1. *Ocotea tenera* $\delta^{18}O$

[30] $\delta^{18}O$ from all four *O. tenera* cores show regular isotope cycles as large as 9‰ (Figure 4). Based on our conceptual model (Figure 1), we assigned the local maxima of each peak to the month of April of each year. Age models were developed individually for each tree (Figure 5), and confirmed based on the sampling date and incremental growth measurements over the last two decades [*Wheelwright and Logan*, 2004]. We were able to detect missing years primarily using these growth observations, and secondarily through identification of apparently truncated cycles in the raw

$\delta^{18}O$ record, a rudimentary crossdating [*Fritts*, 1976] between the four cores, and the results of the forward model simulations. These missing years are not obviously associated with any climatic cause, however, nor are they common among the four cores from the experimental plots. Replicated records from different trees enable the identification of growth hiatuses, but unlike traditional dendrochronological techniques potential age model errors need to be estimated as such replication is still comparatively low.

[31] Annual radial growth increments calculated from the age modeled $\delta^{18}O$ chronologies match those from the basal diameter measurements [*Wheelwright and Logan*, 2004]. The mean of the radial growth rate from sample NWT01A is 4.5 mm year^{-1}, while the estimate from basal diameter measurements is 5.4 mm year^{-1}. The overall mean growth rate from tree NWT02 is 4.3 mm year^{-1} from the age modeled isotope time series, and approximately 4.4 mm year^{-1} from the repeated diameter measurements. Tree NWH03A from the Hoges plot has a $\delta^{18}O$ derived mean growth rate of 4.6 mm year^{-1} and 4.4 mm year^{-1} from observations. The mean interseries correlation [cf. *Fritts*, 1976] between the monthly $\delta^{18}O$ series for the three trees is 0.75, and 0.68 when the amplitudes of the annual cycles are compared. The samples from the Trostles plot are better correlated with one another than with the single core from the Hoges plot, almost entirely because NWH03A does not show the reduction in growth rate and $\delta^{18}O$ amplitude after
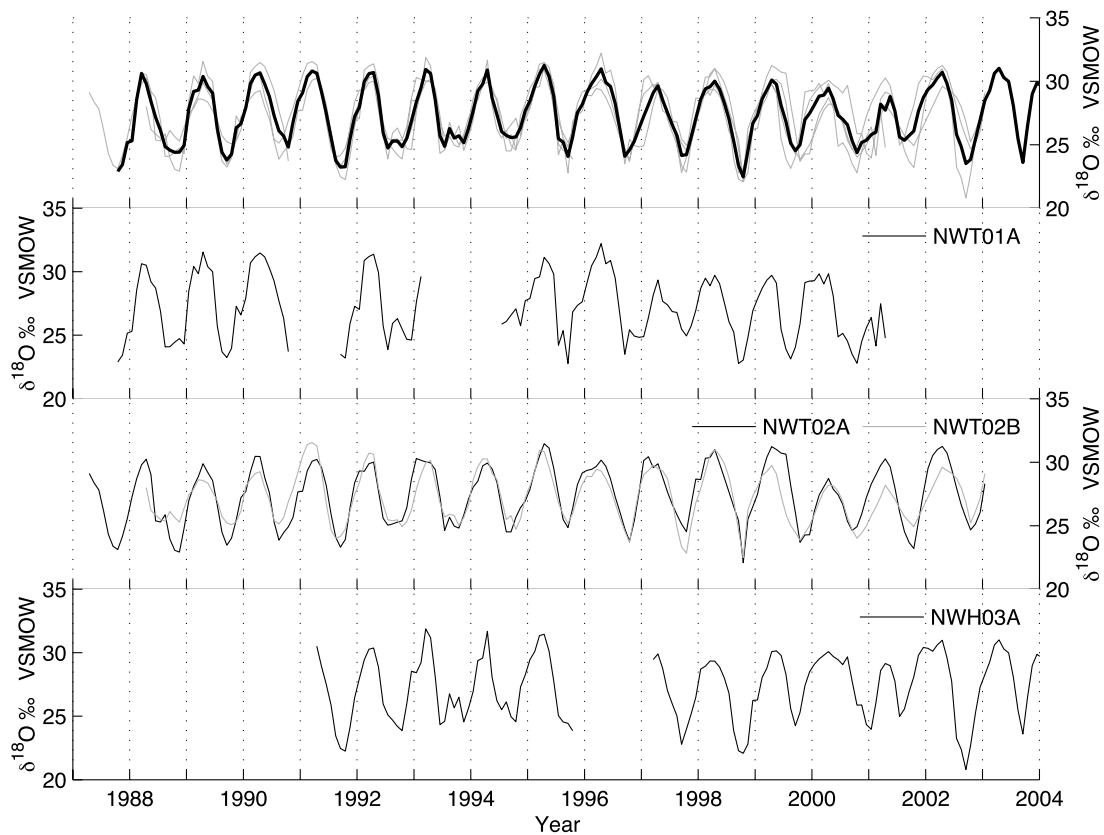
Figure 5. Isotope ratios as a function of time for the four *O. tenera* from the Trostles and Hoges plots. "Missing" years in the age model chronologies reflect both known growth hiatuses from the annual diameter measurements [*Wheelwright and Logan*, 2004] and their confirmation with rudimentary cross-dating between cores and is supported by the results of forward modeling. The top panel shows the mean chronology from all trees (in black) with the individual isotope series in gray.

1999 observed in the older trees from the Trostles plot (see below).

[32] There are some notable features in the $\delta^{18}O$ series as a function of depth. Cores NWT02A and NWT02B, although from the same trees, show different mean growth rates, although in combination their average growth rate is very similar to observations. At least two cores show evidence of a reduced cycle amplitude near the center of the tree, with NWH03A showing a clear plateau in $\delta^{18}O$ and a subsequent resumption of regular cycles. Both the variance reduction and plateau are likely related to either passing through the pith, or as a result of sampling tangential to the growth radius near the center of the tree. At least three out of the four cores (NWT01, NWT02A, and NWT02B) also show growth reductions in the outer-most 10 mm of growth. This is also consistent with the basal growth observations from *Wheelwright and Logan* [2004], which show a clearly reduced growth rate (as small as 2.2 mm year^{-1} in NWT01A) after 1997. A suppression of the amplitude of the annual $\delta^{18}O$ cycle is also observed in the most recent xylem growth.

[33] The mean annual $\delta^{18}O$ cycle from each of the individual trees has the same amplitude within the instrumental precision of measurements (Figure 6a). The seasonal maximum is set by the age model to April, while the annual mean minimum is in September for NWT01A and

NWH03A, and in October for NWT02. These correspond to the peak of the climatological dry and wet seasons, respectively. The composite mean time series formed from the overlapping portions (1991–2001) of the time series of each core shows an average annual cycle of 5.72‰. The $\delta^{18}O$ chronology shows patterns of interannual variability as anomalous amplitude in the annual cycles, ranging from 2.40‰ to 7.55‰ and a standard deviation of 1.45‰ (Figure 6b).

[34] The interannual variability in annual cycle amplitude is driven primarily by a combination of year-to-year changes in the annual minimum value ($\sigma = 0.95$‰) and a declining trend in the value of the annual cycle maximum, most clearly influenced by a decrease after 1996 (Figure 6c), which accounts for the majority of the variance in the annual maxima. Interannual variability in $\delta^{18}O$ is most clearly linked to precipitation (Figure 6d), with wet season precipitation anomalies showing a clear association with linearly detrended amplitude anomalies and a significant relationship that explains more than 50% of the variance, despite the small degrees of freedom ($r = 0.74$, $R^2 = 0.56$, $p < 0.01$). The declining trend in maximum annual $\delta^{18}O$ values mirrors somewhat the declining trends in Monteverde maximum temperature [*Pounds et al.*, 2006]. The decline in maximum $\delta^{18}O$ after 1996 (Figure 6c) in the composite *O. tenera* time series may also reflect the slight increase seen in the relative
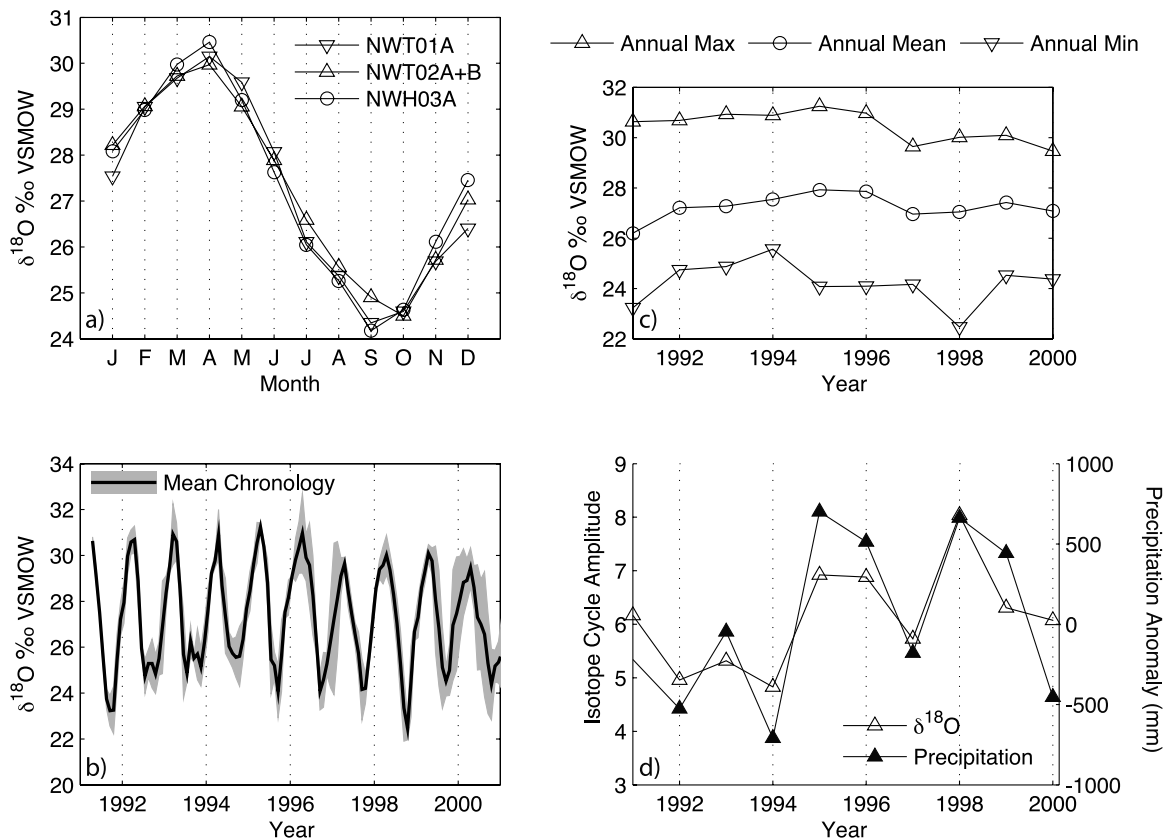
Figure 6. Composite isotope time series for the Trostles/Hoges calibration set. (a) Mean $\delta^{18}O$ annual cycle ("climatology") for the three trees and the mean of all trees. The amplitude and seasonal patterns are indistinguishable within measurement precision, with temporal age model differences of approximately 1 month. (b) Composite time series mean of the three trees (four cores), showing variability (1σ) around the overall mean. (c) Annual maxima, minima, and mean values from the composite mean site chronology. Most of the interannual variability is related to the minima, while the trend in the mean is a result of patterns observed in the annual maxima. (d) The amplitude of the mean annual $\delta^{18}O$ cycle, which shows a clear relationship to interannual patterns in the wet season rainfall ($R^2 = 0.56$, $p < 0.01$, $df = 10$).

humidity corresponding to the location of Monteverde from the NCEP II reanalysis (Figure 3). However, the individual $\delta^{18}O$ series maxima at the calibration site do not in turn mirror the large interannual dry season anomalies seen in the temperature and relative humidity data in, for example, 1992 and 1998 (Figure 3).

4.2. Forest Canopy Trees

[35] Whereas all four *O. tenera* samples showed distinct, large magnitude changes in $\delta^{18}O$ associated with annual changes in precipitation, pilot samples from forest trees showed a range of temporal stable oxygen isotope patterns, most without consistent annual isotope cycles. Of the nine pilot forest trees examined here, five (MV03, MV05, MV12, MV14, and MV15) showed periodic indications of annual cyclicity in $\delta^{18}O$ than could be used for chronology.

[36] *Quercus* might have been an excellent candidate genus for tropical isotope dendroclimatology, because it is relatively common, is straightforward to identify in the field, and is a long-lived mature canopy tree. However, neither of the two samples from *Quercus*, one at 1540 m and the other higher in $\delta^{18}O$ the cloud forest at 1660 meters,

shows consistent cycles in that could be used for chronological control. The lower forest *Quercus* sample (MV05) shows periods of identifiable cyclicity, but much longer periods with no coherent temporal pattern for chronology. The upper cloud forest oak (MV11) shows no detectable $\delta^{18}O$ cycles at all. Similarly, our pilot sample (MV14B) from *Podocarpus* shows short periods of coherent large magnitude changes comparable to those from the experimental plot calibration set, but sustained periods with no detectable cycles in $\delta^{18}O$. Samples from a *Sideroxylon* (MV23A, Sapotaceae) from ~1500 m showed no apparent coherent $\delta^{18}O$ cycles in pilot isotopic measurements. A individual Lauraceae (MV03) had cycles which could be detected for approximately 12 years. However, the tree appears to have experienced extremely suppressed growth in the most recent period (0 to 18 mm depth), making it impossible to tie the chronology to the meteorological record and develop an absolute chronology. Moreover, an individual Lauraceae of the same species growing at the same location (MV02) showed no obvious signs of annual $\delta^{18}O$ cycles. The most promising evidence of species with regular, coherent cycles were from the genus *Pouteria* in the
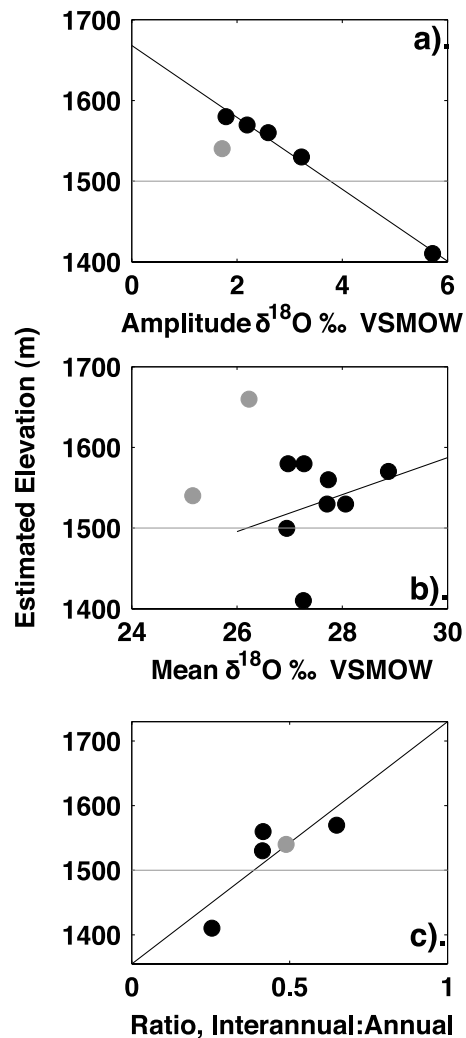
Figure 7. Observed relationships between elevation, $\delta^{18}O$ mean, and the amplitude of the annual $\delta^{18}O$ cycle. (a) Amplitude of the annual cycle (including data from MV03, MV05, MV12, MV14, and MV15; see text for details) and (b) overall mean $\delta^{18}O$ versus elevation. (c) The ratio of the interannual amplitude variance to the mean isotope climatology increases with elevation, showing greater year-to-year climate variability above the orographic cloud bank (indicated by the horizontal line in (a–c), although the actual position will vary at timescales from hours to millennia and longer). Data from *Quercus* (MV05 and MV11) are shown in gray.

Sapotacae family. Samples from this tree (MV12A and MV15C) showed coherent annual cycles over their entire length.

[37] There is a distinct and statistically significant pattern ($R^2 = 0.99$, $p < 0.01$, $n = 5$) associated with elevation in the mean amplitude of the annual cycle in trees (MV05, MV14B, MV03, MV12A, and MV15C) in those instances where it could be detected (Figure 7a). Annual mean $\delta^{18}O$ amplitude ranges from 5.72‰ for the experimental plots at approximately 1410 m to 1.79‰ for sample MV15C at approximately 1580 meters. The lower forest oak (MV05) appears to have cycles of, on average, 1.72‰. Both of the

oak samples (MV05 and MV11) show lower overall mean $\delta^{18}O$ values and MV05 has a suppressed annual cycle amplitude compared with those at similar elevations. There is also an increasing but statistically insignificant trend in total mean $\delta^{18}O$ value with increasing altitude in the Monteverde Cloud Forest (Figure 7b). The two oak trees both show lower average $\delta^{18}O$ with respect to elevation, and overall, than any of the experimental plot or forest trees. The ratio of the standard deviation of the annual amplitude to the mean annual $\delta^{18}O$ cycle increases with elevation, indicating that as the annual cycle is reduced with increasing elevation, the magnitude of the year-to-year variability (anomalies) with respect to the annual cycle increases and a greater proportion of the total variability is in the interannual or longer timescales (Figure 7c).

4.3. Forward $\delta^{18}O$ Modeling

[38] Simulations using our forward model produce annual cycles similar to those seen in the measured $\delta^{18}O$ from the *O. tenera* trees (Figures 8a–8b). The best match between overall variance in the simulated and actual isotope chronologies for the experimental plot trees is achieved using a soil water mixing ratio of approximately 30:70 (30% new precipitation mixing with 70% of the previous month's soil water), although the patterns of interannual isotopic variability are largely insensitive by this choice. Using the Campbell meteorological data, including the derived relative humidity series, the observed and modeled chronologies are significantly correlated ($r = 0.73$, $R^2 = 0.52$, $p < 0.01$), taking into account the high degree of serial autocorrelation ($ar(1, 2)_{obs} = [0.83, 0.45]$, $ar(1, 2)_{model} = [0.77, 0.46]$) in both series [*Ebisuzaki*, 1997]. Simulations using the NCEP Reanalysis II relative humidity (Figure 8) for the grid cell associated with Monteverde are similarly correlated ($r = 0.74$, $R^2 = 0.55$, $p < 0.01$), but are not significantly different. This is largely because the correlation between the simulations and the observed $\delta^{18}O$ time series reflects the large proportion of the total variance in the annual cycle, which is predominantly controlled by the seasonal amount effect reflected in all *O. tenera*. Overall, there is no statistically significant (two-tailed *t*- and *F*-test, $\alpha = 0.05$) difference in the means or variances of the residuals (*observed* − *modeled*) using either NCEP or Campbell-derived relative humidity.

[39] The observed and modeled annual amplitude show similar patterns, but are weakly correlated at this scale (NCEP %RH: $r_{[model,obs]} = 0.55$, $p = 0.08$; Campbell %RH: $r_{[model,obs]} = 0.51$, $p = 0.11$), largely influenced in both cases by the mismatch between the measured and simulated values for 1991 (Figure 8b). The modeled isotope amplitude is significantly correlated over the same period with wet season precipitation anomalies (model using NCEP %RH: $r_{[model,precip]} = 0.71$, $p < 0.01$; model using Campbell %RH: $r_{[model,precip]} = 0.91$, $p < 0.01$), with a substantially stronger correlation between precipitation anomalies and the simulation using the lower amplitude Campbell derived RH record. A downward trend in the annual maximum $\delta^{18}O$ values similar to that observed in our isotope chronology is also seen for model simulations, irrespective of the relative humidity input used, and which appears to result from a combination of increased wet season precipitation and decreased dry season temperatures.
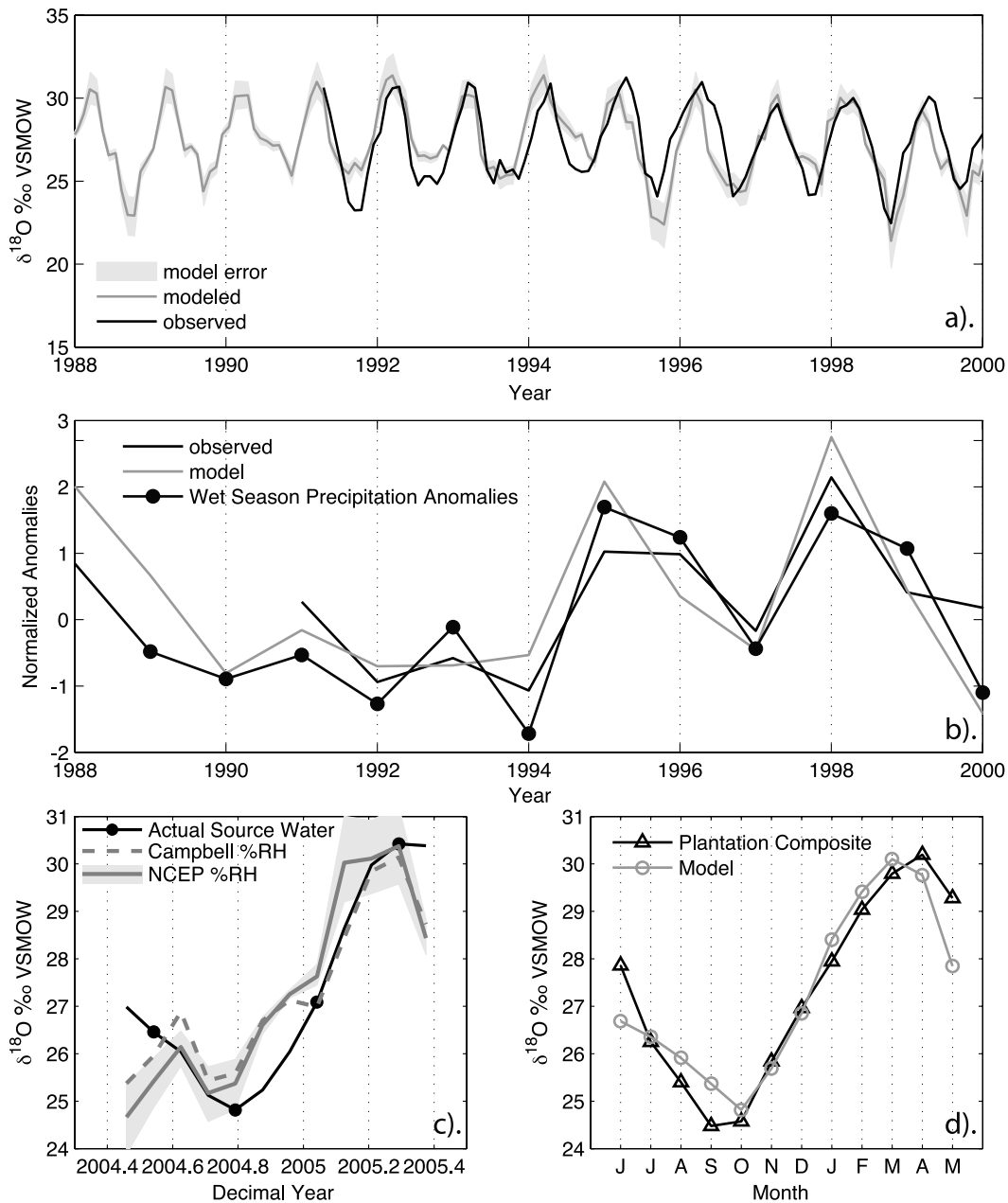
Figure 8. Comparison between observed composite mean *O. tenera* isotope time series and forward model simulation [*Barbour et al.*, 2004; *Evans*, 2007]. Input to the model was observed precipitation and temperature from Monteverde [*Pounds et al.*, 1999], and the mean monthly relative humidity from the NCEP/NCAR reanalysis [*Kanamitsu et al.*, 2002]. (a) The simulated isotope time series is significantly correlated with the observed $\delta^{18}O$ from the experimental plot trees ($r = 0.74$, $R^2 = 0.55$, $p < 0.01$). (b) Observed and modeled chronologies are correlated with wet season precipitation anomalies ($r_{obs} = 0.75$, $p < 0.01$; $r_{model} = 0.71$, $p < 0.01$). (c) The source water model and actual source water produce annual cycle of similar magnitude, and the magnitude of the modeled annual cycle is similar irrespective of the relative humidity data set. (d) The seasonal patterns and isotope climatology of the mean adjusted oxygen isotope climatology are also similar, with an estimated age model error of 1 month.

The NCEP data results in a slightly better match to the actual, observed isotope time series, particularly the annual maxima $\delta^{18}O$ values. The simulated chronology that results from using this data set, however, has larger positive excursions in maximum annual $\delta^{18}O$ that are not seen in the actual chronology (1992, 1994), and results in a overall mean value approximately 1.35‰ enriched above that of the simulation using the Campbell derived relative humidity if the simulations are not adjusted to the observed mean. These differences indicate a model sensitivity of approxi-

mately −0.20‰ for every percent increase in relative humidity.

[40] When compared over the limited period for which both climate data and volume-weighted seasonal $\delta^{18}O$ of meteoric waters at Monteverde are available, the forward model simulations using calculated and observed source water isotope ratios show similar seasonal patterns and amplitudes (Figure 8c). The amount effect model (equation 5) reproduces the seasonal pattern of observed meteoric water $\delta^{18}O$ on which it was based, with a slight loss of variance at the annual maxima and minima (Figure 8c). The modeled α-cellulose $\delta^{18}O$ cycle amplitude is also similar whether observed or modeled source water is used, and irrespective of the relative humidity data set. However, uncertainties in model parameters can result in a confidence interval up to 1.5‰ wide, particularly at the local maxima and minima of the simulated annual $\delta^{18}O$ cycles. The seasonal pattern and mean annual isotope cycle in both simulated and observed *O. tenera* are quite similar, with an apparent age model bias of ±1 month (Figure 8d). Some of this phase offset could be due to the necessary but probably simplistic assumption that growth rates are constant over the course of a year. In the absence of more frequent basal measurements, however, this assumption is reasonable and moreover does not influence our climatic interpretations.

5. Discussion

5.1. Annual Oxygen Isotope Cycles

[41] Annual $\delta^{18}O$ cycles are clearly present in our set of *O. tenera* trees, and are sufficiently large and well defined that they are easily distinguished from the occasional smaller positive excursions at the time of the annual minima, which are probably the result of the existence and magnitude of the Central American midsummer (July and August) drought, which can be seen in some years (i.e., 1993) in both the observed and modeled α-cellulose $\delta^{18}O$ time series. The similarity between the measured radial growth rates from long-term monitoring and those derived from the age modeled isotope time series, and supported by the forward model simulations, demonstrates conclusively that the proxy $\delta^{18}O$ chronology can be securely established using these cycles. Even given the potential uncertainties associated with both individual repeated basal growth measurements [*Sheil*, 2003; *McLaughlin et al.*, 2003] and the increment estimates from age modeled $\delta^{18}O$, the consistency between the two data sets indicates the age model (1 cycle = 1 year) is particularly robust. There is no indication from the isotope time series that the *Ocotea tenera* have a significant regular growth hiatus during the year, which is supported by comparison to our forward modeling results.

[42] Unlike traditional dendroclimatological approaches using tree ring widths or density, where massive sample replication and robust crossdating result in an overall composite age model error that is effectively negligible [*Fritts*, 1976], the smaller sample depth and limited opportunity for crossdating in our experimental plot $\delta^{18}O$ chronology leaves open the possibility of error in assigning the isotope time series to calendar years. This is exacerbated here by the short length of the chronologies developed from our calibration set. Even in our *O. tenera* calibration

samples, development of the age model is complicated by years where individual trees did not have appreciable basal growth, the reduced growth rates since ∼1997, and gaps in the annual observational data. This latter factor is particularly important between 1997 and 2002, because sometime between 2001 and 2004 all basal growth in several trees in Trostles plot had ceased or slowed to imperceptible increments. For our *O. tenera* chronology, we estimate an age model error no larger than ±2 years, based on the basal growth measurements and comparison with the forward model simulations. In unmonitored trees and particularly in trees growing at average rates less than 2 mm year^{-1}, age model error might be determined by the range of possible realistic age models, and may be complemented by high-resolution radiocarbon assays on the period since A.D. 1955 [*Worbes and Junk*, 1989]. Unfortunately, while the *O. tenera* in the experimental plots allow us to test and calibrate our proposed age model and detect the imprint of climate variability on the $\delta^{18}O$ cycles, this early successional species is unlikely to provide the material for long isotope chronologies.

[43] There are several factors which could potentially complicate identification of annual isotope cycles. Long residence times for meteoric waters in the soil would result in temporal mixing of different seasonal water sources, which would both smooth and dampen the amplitude of the annual signal we seek for chronological control. Likewise, trees which access primarily deeper sources of groundwater would be relatively insensitive to the intra-annual change in the $\delta^{18}O$ of available moisture [cf. *Evans and Schrag*, 2004]. However, shallow rooting depths for cloud forest trees [*Matelson et al.*, 1995] in response to soil nutrient availability should mean that shallow soil water is their primary moisture source and they do not have access, or need to access, deeper groundwaters. However, one alternative hypothesis for the lack of annual cycles in some of the forest trees analyzed here is that they are indeed able to access deeper groundwater or well-mixed stream waters, and are relatively insensitive to the seasonal $\delta^{18}O$ cycle of meteoric waters.

[44] At the sampling resolution used in this study and given requirements for minimum α-cellulose yield, growth rates had to be sufficiently rapid, ∼2 mm per year, to allow for enough samples per year in order to sufficiently resolve the annual cycle and its amplitude, but not so rapid as to limit the ultimate length of the reconstruction. Slower growth rates make it difficult to resolve the full amplitude of the annual cycle given current analytical constraints. This can be partially addressed by using larger-diameter increment borers, whole cross-sections, or improved analytical procedures that require less cellulose for a precise measurement. Already, improvements in the techniques and technologies described and used here have reduced the amount of α-cellulose required for precise $\delta^{18}O$ measurements [*Evans*, 2008].

[45] There is an upward trend in the mean oxygen isotope ratio with elevation for all the trees (experimental plots and forest trees), when *Quercus* is excluded. While the trend is not statistically significant, it suggests that higher elevation trees may on average use more ^{18}O-enriched cloud water, which would be consistent with their position progressively closer to the continental divide and within the region of persistent cloud. *Quercus* appears to be a different case,

with overall mean $\delta^{18}O$ values substantially lower than other species, and a smaller average amplitude in MV05. Collectively, these data suggest that our *Quercus* preferentially sample soil water with a more negative $\delta^{18}O$. This could arise if the trees did not add basal growth during part of the transition or dry season, when $\delta^{18}O$ values are higher. If *Quercus* ceased growth during part of the dry season, both the mean isotopic value and the annual cycle, where present, would preferentially reflect the more negative $\delta^{18}O$ during the rainy season. Alternatively, this species may have access to some deeper soil water sources, which would also explain the suppressed amplitude of the mean annual cycle. Finally, if transpiration were more restricted in *Quercus*, potentially through particular physiological characteristics or structure of the leaves, enrichment of the source water in the leaves would be limited and the resultant cellulose would have a more negative $\delta^{18}O$ value. In general, though there are several possible reasons why some of the forest trees studied here do not display annual cycles, the simplest cause may be that our sampling interval of 200 μm failed to adequately resolve the annual cycle in very slow growing trees.

[46] Two robust features characterize the annual cycles in the forest trees considered here. The amplitude of the annual cycle decreases with elevation, and the ratio of the variance in the interannual amplitude to the mean annual cycle amplitude increases. The reduction in the amplitude of the annual cycle is likely related to longer soil water residence times and increased mixing of seasonal water sources, which in turn is probably a result of lower temperatures, increased cloud cover, and reduced solar irradiance at higher elevations within the orographic cloud bank. The increase in the ratio of the interannual cycle anomaly to the annual amplitude indicates that the higher elevation trees may be more sensitive to year-to-year variability than trees from the lower premontane forest. There are indications that this is related in some trees to larger interannual variations in the annual cycle maxima.

5.2. Climate Analysis

[47] Interannual anomalies in the amplitude of the *O. tenera* $\delta^{18}O$ cycles are dominated by variability in the annual minima value, which in agreement with our conceptual model (Figure 1) is primarily controlled by the amount of rainfall received during the wet season (Figure 6d). There is little year-to-year variance in the annual maxima in the composite mean $\delta^{18}O$ series from the experimental plots, with a small downward trend related primarily to a slight step change between 1996 and 1997. This downward trend might be related to increases in relative humidity or decreases in maximum temperatures [*Pounds et al.*, 2006] over the common period, but missing from the $\delta^{18}O$ maxima are distinct large positive anomalies which could be related to interannual temperature or relative humidity anomalies associated with El Niño events.

[48] The most likely reason for the lack of a clear dry season $\delta^{18}O$ anomaly signal in the *O. tenera* series is the elevational position of our pilot calibration site at ~1410 m in the transitional region between premontane wet and cloud forest. At this lower elevation, the persistent cloud immersion that characterizes forests along the continental divide above 1500 m is considerably reduced, although mist can

still be an important moisture source for vegetation. Trees in the premontane wet forest and below the mean lifting condensation level would be relatively insensitive to changes in orographic cloud base height and relative humidity since the magnitude of the local hydroclimatic alterations to fluctuations would therefore be relatively small. At higher elevations above the mean lifting condensation level, where forests are on average consistently within or at the margin of the prevailing orographic cloud bank, fluctuations between cloud and cloud-free conditions would be accompanied by rather large local changes in temperature, relative humidity, water vapor, and solar irradiance. Support for this interpretation comes from analysis of the canopy trees in which annual cycles were detected. In 3 out of the 5 forest trees with annual cycles, variance in annual maxima is greater than the annual minima.

[49] Additional complicating factors may arise from the heterogeneous nature of cloud cover [*Clark et al.*, 2000; *Haber*, 2000; *Guswa et al.*, 2007]. Gaps in the cordillera can allow orographic clouds to pass to lower elevations on the leeward side, often along stream courses. Likewise, topography may dictate the extent to which individual trees are exposed to direct tradewind moisture advection, and soil type and depth may influence the amount of source water buffering and soil water mixing that determines the baseline amplitude for the formation of annual $\delta^{18}O$ cycles.

[50] There are indications that higher elevation trees show a greater sensitivity to year-to-year variability, particularly to dry season climate likely related to the influence of orographic clouds. This suggests that optimal sampling locations for reconstructing both cloudiness and the regional scale forcing associated with changes in cloud coverage and moisture advection will be at those elevations where the annual cycle is coherent and of a sufficient magnitude to be differentiated from short term fluctuations, but where high-frequency variance suggests sensitivity to these changes. Based on our pilot samples from forest canopy trees, Sapotaceae from the high elevation cloud forest may hold the most promise for the development of long paleoclimate records.

5.3. Forward Modeling

[51] The 14 environmental parameters from the model of *Barbour et al.* [2004] are assumed to be temporally stable [*Evans*, 2007], and therefore changes in the parameter set are predominantly reflected by changes in the overall mean of the series, and secondarily in the amplitude of the isotope time series. For instance, a change in the constrained effective length parameter (L, which controls the Peclet number φ) of 1 mm can change both the mean and variance of the resulting isotope time series by approximately 0.4‰; however, even large changes in this parameter [*Barbour et al.*, 2004] do not significantly change the pattern of year-to-year variability nor the seasonal cycle. Therefore while both the mean and variance of the simulated $\delta^{18}O$ chronology can be influenced by uncertainty in model parameters, the seasonal and interannual patterns are predominantly driven by the meteorological data themselves. The results from Figure 8c demonstrate that the interannual difference in the annual amplitude of the $\delta^{18}O$ cycle imparted by uncertainties in the model parameter set may be as large as 1.5‰, but this is almost entirely due to an overall inflation or dilation

of the time series variance. Additional uncertainty arises from the derived amount effect relationship, which accounts for only 56% of the observed isotopic variation in precipitation. Additional influences on precipitation $\delta^{18}O$ probably include enrichment due to re-evaporation from the land surface [*Rhodes et al.*, 2006] and source isotopic composition, neither of which are captured by our regression model. In agreement with the findings of *Evans* [2007], however, we find that the overall structure and mean amplitude of the annual cycle is driven predominantly by the seasonal change in the $\delta^{18}O$ related to changes in water sources as controlled primarily by the amount effect and, in this case, the additional contribution of cloud water during the dry season. It is clear, however, from interannual differences observed between model simulations using the two different relative humidity data sets, that differences in the input data can have an important influence on interannual patterns of variability. In general, neither relative humidity data set produces a substantially improved overall match to the observed experimental plot $\delta^{18}O$ time series.

[52] More interesting is the disparity between the correlations with each simulation and wet season anomalies. Modeled $\delta^{18}O$ values using the NCEP relative humidity data set show a weaker correlation with precipitation anomalies than the $\delta^{18}O$ time series simulated from the calculated Campbell relative humidity, although the coefficient is more similar to the relationship between the observed *O. tenera* $\delta^{18}O$ and wet season precipitation. This indicates that increased variability in relative humidity can have a substantial influence on the controls on the interannual patterns of variability. This suggests that samples within or at the boundary of the orographic cloud bank are likely to show great sensitivity to, and control by, changes in relative humidity and leeward-slope moisture advection than those below it. This finding, and the observations of increasing interannual variability relative to the mean annual $\delta^{18}O$ with increases in elevation, will be used to guide future sampling strategies for the development of long chronologies.

[53] In *Evans* [2007], the *Barbour et al.* [2004] model was used to construct the interannual variability in the amplitude of the seasonal cycle, while the mean and variance were scaled to that of the observed $\delta^{18}O$ time series. Here using the default parameterization from *Evans* [2007], even without mean adjustment, and using the relative humidity derived from the Campbell meteorological data [*Pounds et al.*, 1999], the model actually reproduces the mean of the series within the precision of the instruments ($\bar{x}_{model} = 26.52‰$, $\bar{x}_{obs} = 26.27‰$), although this may simply be fortuitous, since as previously discussed large shifts in the overall mean can be the result of changing the model and source water parameters. The use of the soil water model in the place of variance adjustment also produced a simulated isotope series with similar mean amplitude and variance as the $\delta^{18}O$ from *O. tenera*, and generally reproduced the visually coherent cyclicity of the actual time series. Most encouragingly, applying the soil water model reproduces the leading autocorrelation structure of the observed $\delta^{18}O$ chronologies, as well as the pattern of interannual variability and the relationship between the annual amplitude anomalies and wet season precipitation amount (Figure 8c).

[54] The monthly mixing ratio of 30:70 (precipitation to prior soil water) implies a mean water residence time somewhat longer than would be calculated from the turnover rate reported from lowland tropical rain forest soils derived from tritium measurements by *McGinnis et al.* [1969] in Panama. However, *McGinnis et al.* [1969] estimated soil water flux for only the top 30 cm. Somewhat deeper soil water available to plants would presumably have a longer residence time. Additionally, reduced evapotranspiration due to persistent cloud cover, cooler temperatures, and higher relative humidity would likely increase water residence times in soils in tropical montane cloud forests.

[55] The most obvious discrepancy between the *O. tenera* composite mean time series, the simulated model, and local climate variability is the wet season minimum of 1991. Although one possible hypothesis is that the age model is incorrect, the 1991 negative anomaly is apparent in the $\delta^{18}O$ from the most securely dated cores, those cores from tree NWT02, and there is no evidence from basal growth analysis to suggest an age adjustment of several years is warranted nor even realistic. Zonal winds across the Costa Rican cordillera were anomalously strong during the wet season in 1991 [*Kanamitsu et al.*, 2002], and high resolution gridded monthly precipitation data for Central America (Universidad Nacional Autónoma de México (UNAM) data from the Centro de Ciencias de la Atmósfera, served from http://iridl.ldeo.columbia.edu/SOURCES/.UNAM/.gridded/ .monthly/.v0705/ at the International Research Institute for Climate and Society (IRI), Columbia University.) also indicate that 1991 was one of the wettest rainy seasons (July through September) over the period 1901 to 2002 for the grid cell corresponding to Monteverde and northwestern Costa Rica, in contrast to the Monteverde rain gauge data.

5.4. Cloud Forest Isotope Dendroclimatology

[56] Our selection of tropical cloud forests as a site for tropical paleoclimate reconstruction parallels, in a somewhat paradoxical manner, the approach of classical dendroclimatology in seeking out sampling locations where trees are likely to be sensitive to relatively small changes in annual climate. In temperate regions and for trees with regular annual changes in morphology or wood density, these are typically dry or cold sites at the limits of a species range. For tropical isotope dendroclimatology, however, we seek sites which are wet enough to allow trees to grow throughout the year, yet are subjected to seasonal changes in the stable oxygen isotope composition of available moisture which provides the means of establishing annual chronology. In cloud forest environments, the largest interannual changes of interest are likely to be wet season rainfall and dry season cloudiness. As such, site selection for tropical isotope dendroclimatology is very different from that of classical field approaches in dendrochronology in terms of climate regimes, but the guiding principle is the same.

[57] Our approach to tropical isotope dendroclimatology [*Evans and Schrag*, 2004] has a closer methodological and procedural affinity to paleoclimate analysis using speleothems or corals than to classical dendrochronology. Despite rapid advances [*Kornexl et al.*, 1999; *Brendel et al.*, 2000; *Evans*, 2008], the analytical requirements for sample preparation and mass spectrometry still limit the number of samples and measurement replication that can be realisti-

cally achieved. The result is relatively large uncertainties (several years) in the age modeled chronologies. However, as demonstrated by *McCarroll and Pawellek* [1998] and *Gagen et al.* [2004], stable isotope ratios in tree ring chronologies often have a higher signal-to-noise ratio that ring width data. As a consequence, fewer chronologies may be required to achieve a robust common signal. For the Monteverde *O. tenera* chronology, 3 trees over the common period of overlap are sufficient to meet an Expressed Population Signal threshold (EPS [*Wigley et al.*, 1984]) of 0.85. Furthermore, the protocols allow for the development of high-resolution terrestrial proxy records that bypasses some of the extant challenges to developing tropical ring width chronologies, and can be applied even when appropriate species for traditional dendrochronology cannot be identified. Application of these techniques will necessarily be guided by the specific research question and the ability of complementary proxies to provide the information necessary to address them. Cloud forests, given their biogeographical and hydrological importance at the regional scale, and their sensitivity to major modes of climate such as El Niño at the global scale [*Loope and Giambelluca*, 1998; *Still et al.*, 1999; *Pounds et al.*, 1999; *Foster*, 2001; *Bush*, 2002; *Pounds et al.*, 2006] represent a particular ecosystem where the application of tropical isotope dendroclimatology can support an improved understanding of critical environmental processes across a range of spatiotemporal scales. Until recently, the relative inaccessibility of tropical cloud forests has spared them from the worst consequences of indiscriminate logging, increasing the likelihood that old trees might persist in these ecosystems throughout the tropics, providing a potential source of long-term paleoclimate information.

6. Summary and Conclusions

[58] The results from our study clearly identify an annual isotope cycle in trees growing in experimental plots at lower cloud forest elevations that can be used to develop an annual chronology in the absence of annual rings. Interannual variability in the amplitude of the annual cycle is associated with wet season precipitation anomalies at our premontane wet forest calibration site. Our forward model simulations successfully reproduce the annual pattern of $\delta^{18}O$ observed in our *O. tenera* trees and demonstrate a similar autocorrelation structure in both synthetic and actual isotope time series. The model also reproduces quite well the dependence of the interannual patterns of $\delta^{18}O$ amplitude on the amount of wet season rainfall. Five mature canopy trees considered here from sites ranging from 1500 to 1660 m also show an annual isotope cycle, and two of these have $\delta^{18}O$ cycles that can be consistently detected over their entire length. Collectively, these pilot results can help guide the future development of long climate reconstructions from older cloud forest trees. The results of our calibration study at Monteverde demonstrate that annual stable oxygen isotope cycles in tropical cloud forest trees can be used for both chronology development and the detection of climate variability, and can be applied to the development of climate reconstructions and the interpretation of recent trends in tropical montane forest hydroclimatology.

References

Anchukaitis, K. J., M. N. Evans, T. Lange, D. R. Smith, D. P. Schrag, and S. W. Leavitt (2008), Consequences of a rapid cellulose extraction technique for oxygen isotope and radiocarbon analyses, *Anal. Chem.*, 80, 2035–2041, doi:10.1021/ac7020272.

Barbour, M. M., U. Schurr, B. K. Henry, S. C. Wong, and G. D. Farquhar (2000), Variation in the oxygen isotope ratio of phloem sap sucrose from Castor Bean. Evidence in support of the Peclet effect, *Plant Physiol.*, 123(2), 671–680, doi:10.1104/pp.123.2.671.

Barbour, M. M., A. S. Walcroft, and G. D. Farquhar (2002), Seasonal variation in $\delta^{13}C$ and $\delta^{18}O$ of cellulose from growth rings of *Pinus radiata*, *Plant Cell Environ.*, 25(11), 1483–1499.

Barbour, M. M., J. S. Roden, G. D. Farquhar, and J. R. Ehleringer (2004), Expressing leaf water and cellulose oxygen isotope ratios as enrichment above source water reveals evidence of a Peclet effect, *Oecologia*, 138(3), 426–435.

Bauch, J., L. Quiros, G. Noldt, and P. Schmidt (2006), Study on the wood anatomy, annual wood increment and intra-annual growth dynamics of *Podocarpus oleifolius* var. *macrostachyus* from Costa Rica, *J. Appl. Bot. Food Qual.*, 80(1), 19–24.

Bradley, R., M. Vuille, H. Diaz, and W. Vergara (2006), Threats to water supplies in the tropical Andes, *Science*, 312(5781), 1755–1756, doi:10.1126/science.1128087.

Brendel, O., P. P. M. Iannetta, and D. Stewart (2000), A rapid and simple method to isolate pure α-cellulose, *Phytochem. Anal.*, 11, 7–10.

Brienen, R., and P. Zuidema (2005), Relating tree growth to rainfall in Bolivian rain forests: A test for six species using tree ring analysis, *Oecologia*, 146(1), 1–12.

Brown, A. D., and M. Kappelle (2001), Introducción a los bosques nublados del neotrópico: Una síntesis regional, in *Bosques nublados del neotrópico*, edited by M. Kappelle and A. D. Brown, pp. 25–40.

Bruijnzeel, L. (1991), Hydrological impacts of tropical forest conversion, *Nat. Resour.*, 27, 36–46.

Bruijnzeel, L. A. (2001), Hydrology of tropical montane cloud forests: A reassessment, *Land Use Water Resour. Res.*, 1, 1–18.

Bruijnzeel, L. A. (2004), Hydrological functions of tropical forests: Not seeing hydrological functions of tropical forests: Not seeing the soil for the trees?, *Agric. Ecosyst. Environ.*, 104, 185–228.

Bruijnzeel, L. A., and J. Proctor (1995), Hydrology and biochemistry of tropical montane cloud forests: What do we really know?, in *Tropical Montane Cloud Forests*, edited by L. Hamilton, J. O. Juvik, and F. N. Scatena, Springer-Verlag, New York.

Bruijnzeel, L. A., and E. J. Veneklaas (1998), Climatic conditions and tropical, montane forest productivity: The fog has not lifted yet, *Ecology*, 79, 3–9.

Buckley, B. M., K. Palakit, K. Duangsathaporn, P. Sanguantham, and P. Prasomsin (2007), Decadal scale droughts over northwestern Thailand over the past 448 years: Links to the tropical Pacific and Indian Ocean sectors, *Clim. Dyn.*, 29(1), 63–71.

Bush, M. B. (2002), Distributional change and conservation on the Andean flank: A palaeoecological perspective, *Global Ecol. Biogeogr.*, 11, 463–473.

Clark, K. L., N. M. Nadkarni, D. Schaefer, and H. L. Gholz (1998), Cloud water and precipitation chemistry in a tropical montane forest, Monteverde, Costa Rica, *Atmos. Environ.*, 32, 1595–1603.

Clark, K. L., R. O. Lawton, and P. R. Butler (2000), The physical environment, in *Monteverde: Ecology and Conservation of a Tropical Cloud Forest*, edited by N. M. Nadkarni and N. T. Wheelwright, pp. 15–38, Oxford University Press, Oxford, U. K.

D'Arrigo, R., R. Wilson, J. Palmer, P. Krusic, A. Curtis, J. Sakulich, S. Bijaksana, S. Zulaikah, and L. O. Ngkoimani (2006), Monsoon

drought over Java, Indonesia, during the past two centuries, *Geophys. Res. Lett.*, 33, L04709, doi:10.1029/2005GL025465.

Dawson, T. E. (1998), Fog in the California redwood forest: Ecosystem inputs and use by plants, *Oecologia*, 117, 476–485.

Diaz, H. F., and N. E. Graham (1996), Recent changes in tropical freezing heights and the role of sea surface temperature, *Nature*, 383, 152–155.

Dünisch, O., J. Bauch, and L. Gasparotto (2002), Formation of increment zones and intraannual growth dynamics in the xylem of *Swietenia macrophylla*, *Carapa guianensis*, and *Cedrela odorata* (Meliaceae), *IAWA J.*, 23, 101–119.

Ebisuzaki, W. (1997), A method to estimate the statistical significance of a correlation when the data are serially correlated, *J. Clim.*, 10(9), 2147–2153.

Evans, M. N. (2007), Toward forward modeling for paleoclimatic proxy signal calibration: A case study with oxygen isotopic composition of tropical woods, *Geochem. Geophys. Geosyst.*, 8, Q07008, doi:10.1029/2006GC001406.

Evans, M. N. (2008), A reactor for high temperature pyrolysis and oxygen isotopic analysis of cellulose via induction heating, *Rapid Commun. Mass Spectrom.*, 22, 2211–2219.

Evans, M. N., and D. P. Schrag (2004), A stable isotope-based approach to tropical dendroclimatology, *Geochim. Cosmochim. Acta*, 68, 3295–3305, doi:10.1016/j.gca.2004.01.0061353.

February, E. C., and W. D. Stock (1998), An assessment of the dendrochronological potential of two *Podocarpus* species, *Holocene*, 8(6), 747.

Feild, T. S., and T. E. Dawson (1998), Water sources used by *Didymopanax pittieri* at different life stages in a tropical cloud forest, *Ecology*, 79, 1448–1452.

Fischer, D. T., and C. J. Still (2007), Evaluating patterns of fog water deposition and isotopic composition on the California Channel Islands, *Water Resour. Res.*, 43, W04420, doi:10.1029/2006WR005124.

Foster, P. (2001), The potential negative impacts of global climate change on tropical montane cloud forests, *Earth Sci. Rev.*, 55, 73–106.

Fritts, H. C. (1976), *Tree Rings and Climate*, Academic Press, New York.

Gagen, M., D. McCarroll, and J. L. Edouard (2004), Latewood width, maximum density, and stable carbon isotope ratios of pine as climate indicators in a dry subalpine environment, French Alps, *Arct. Antarc. Alp. Res.*, 36, 166–171.

Gat, J. R. (1996), Oxygen and hydrogen isotopes in the hydrologic cycle, *Annu. Rev. Earth Planet. Sci.*, 24, 225–262.

Gonfiantini, R., M.-A. Roche, J.-C. Olivy, J.-C. Fontes, and G. M. Zuppi (2001), The altitude effect on the isotopic composition of tropical rains, *Chem. Geol.*, 181(147–167).

Guswa, A. J., A. L. Rhodes, and S. E. Newell (2007), Importance of orographic precipitation to the water resources of Monteverde, Costa Rica, *Adv. Water Res.*, 30(10), 2098–2112, doi:10.1016/j.advwatres.2006.07.008.

Haber, W. A. (2000), Plants and vegetation, in *Monteverde: Ecology and Conservation of a Tropical Cloud Forest*, edited by N. M. Nadkarni and N. T. Wheelwright, pp. 39–70, Oxford Univ. Press, Oxford, U. K.

Hamilton, L. S., J. O. Juvik, and F. N. Scatena (Eds.) (1995), *Tropical Montane Cloud Forests*, Springer-Verlag.

Holder, C. D. (2004), Rainfall interception and fog precipitation in a tropical montane cloud forest of Guatemala, *For. Ecol. Manage.*, 190, 373–384.

Ingraham, N. (1998), Isotopic variations in precipitation, in *Isotope Tracers in Catchment Hydrology*, edited by C. K. J. McDonnell, Elsevier Press, Amsterdam, Netherlands.

Ingraham, N., and R. Matthews (1990), A stable isotopic study of fog - the Point Reyes Peninsula, California, USA, *Chem. Geol.*, 80, 281–290.

Ingraham, N. L., and R. Matthews (1995), The importance of fog-drip water to vegetation - Point Reyes Peninsula, California, *J. Hydrol.*, 164(1–4), 269–285.

Jarvis, P. G., and K. G. McNaughton (1986), Stomatal control of transpiration: Scaling up from leaf to region., *Adv. Ecol. Res.*, 15, 1–50.

Kanamitsu, M., W. Ebisuzaki, J. Woollen, S. Yang, J. Hnilo, M. Fiorino, and G. Potter (2002), NCEP-DOE AMIP-II Reanalysis (R-2), *Bull. Am. Meteorol. Soc*, 83(11), 1631–1643.

Kapos, V., and E. V. J. Tanner (1985), Water relations of Jamaican upper montane rain forest trees, *Ecology*, 66(1), 241–250.

Kornexl, B. E., M. Gehre, R. Höfling, and R. A. Werner (1999), On-line $\delta^{18}O$ measurement of organic and inorganic substances, *Rapid Commun. Mass Spectrom.*, 13, 1685–1693.

Lachniet, M. S., and W. P. Patterson (2002), Stable isotope values of Costa Rican surface waters, *J. Hydrol.*, 260, 135–150.

Lawton, R. O., U. S. Nair, R. A. Pielke, and R. M. Welch (2001), Climatic impact of tropical lowland deforestation on nearby montane cloud forests, *Science*, 294, 584–587.

Linacre, E. (1964), A note on a feature of leaf and air temperatures, *Agric. Meteorol.*, 1(1), 66–72.

Loope, L. L., and T. W. Giambelluca (1998), Vulnerability of island tropical montane cloud forests to climate change, with special reference to East Maui, Hawaii, *Clim. Change*, 39, 503–517.

Magaña, V., J. A. Amador, and S. Medina (1999), The midsummer drought over Mexico and Central America, *J. Clim.*, 12(6), 1577–1588.

Matelson, T. J., N. M. Nadkarni, and R. Solano (1995), Tree damage and annual mortality in a montane forest in Monteverde, Costa Rica, *Biotropica*, 27, 441–447.

McCarroll, D., and F. Pawellek (1998), Stable carbon isotope ratios of latewood cellulose in *Pinus sylvestris* from northern Finland: Variability and signal-strength, *Holocene*, 8(6), 675–684.

McGinnis, J. T., F. B. Golley, R. G. Clements, G. I. Child, and M. J. Duever (1969), Elemental and hydrologic budgets of the Panamanian tropical moist forest, *Bioscience*, 19(8), 697–700.

McLaughlin, S. B., S. D. Wullschleger, and M. Nosal (2003), Diurnal and seasonal changes in stem increment and water use by yellow poplar trees in response to environmental stress, *Tree Physiol.*, 23, 1125–1136.

Nadkarni, N. M., and N. T. Wheelwright (Eds.) (2000), *Monteverde: Ecology and Conservation of a Tropical Cloud Forest*, Oxford Univ. Press, Oxford, U. K.

Nair, U. S., R. O. Lawton, R. M. Welch, and R. A. Pielke Sr. (2003), Impact of land use on Costa Rican tropical montane cloud forests: Sensitivity of cumulus cloud field characteristics to lowland deforestation, *J. Geophys. Res.*, 108(D7), 4206, doi:10.1029/2001JD001135.

Pounds, J. A., M. Fogden, and J. H. Campbell (1999), Biological response to climate change on a tropical mountain, *Nature*, 398, 611–615.

Pounds, J. A., et al. (2006), Widespread amphibian extinctions from epidemic disease driven by global warming, *Nature*, 439(7073), 161–167.

Rhodes, A. L., A. J. Guswa, and S. E. Newell (2006), Seasonal variation in the stable isotopic composition of precipitation in the tropical montane forests of Monteverde, Costa Rica, *Water Resour. Res.*, 42, W11402, doi:10.1029/2005WR004535.

Robertson, I., C. A. Froyd, R. P. D. Walsh, D. M. Newbery, S. Woodborne, and R. C. Ong (2004), The dating of dipterocarp tree rings: Establishing a record of carbon cycling and climatic change in the tropics, *J. Quat. Sci.*, 19, 657–664.

Roden, J. S., G. Lin, and J. R. Ehleringer (2000), A mechanistic model for interpretation of hydrogen and oxygen ratios in tree-ring cellulose, *Geochim. Cosmochim. Acta*, 64, 21–35.

Root, T. L., J. T. Price, K. R. Hall, S. H. Schneider, C. Rosenzweig, and J. A. Pounds (2003), Fingerprints of global warming on wild animals and plants, *Nature*, 421, 57–60.

Schmid, S. (2004), Water and ion fluxes to a tropical montane cloud forest ecosystem in Costa Rica, Master's thesis, University of Bern.

Scholl, M. A., T. W. Giambelluca, S. B. Gingerich, M. A. Nullet, and L. L. Loope (2007), Cloud water in windward and leeward mountain forests: The stable isotope signature of orographic cloud water, *Water Resour. Res.*, 43, W12411, doi:10.1029/2007WR006011.

Sheil, D. (2003), Growth assessment in tropical trees: Large daily diameter fluctuations and their concealment by dendrometer bands, *Can. J. For. Res.*, 33(10), 2027–2035.

Stadtmüller, T. (1987), *Cloud forests in the humid tropics*, United Nations University.

Still, C., P. Foster, and S. Schneider (1999), Simulating the effects of climate change on tropical montane cloud forests, *Nature*, 398, 608–610.

Therrell, M. D., D. W. Stahle, L. P. Ries, and H. H. Shugart (2006), Tree-ring reconstructed rainfall variability in Zimbabwe, *Clim. Dyn.*, 26(7), 677–685.

van Dijk, A., and L. Bruijnzeel (2001), Modelling rainfall interception by vegetation of variable density using an adapted analytical model: Part 2. Model validation for a tropical upland mixed cropping system, *J. Hydrol.*, 247, 239–262.

Wheelwright, N. T., and A. Bruneau (1992), Population sex ratios and spatial distribution of *Ocotea tenera* (Lauraceae) trees in a tropical forest, *J. Ecol.*, 80(3), 425–432.

Wheelwright, N. T., and B. A. Logan (2004), Previous-year reproduction reduces photosynthetic capacity and slows lifetime growth in females of a neotropical tree, *Proc. Natl. Acad. Sci.*, 101(21), 8051–8055.

Wigley, T. M. L., K. R. Briffa, and P. D. Jones (1984), On the average value of correlated time series, with applications in dendroclimatology and hydrometeorology, *J. Clim. Appl. Meteorol.*, 23, 201–213.

Worbes, M. (2002), One hundred years of tree-ring research in the tropics - a brief history and an outlook to future challenges, *Dendrochronologia*, 20(1–2), 217–231.

Worbes, M., and W. Junk (1989), Dating tropical trees by means of C14 from bomb tests, *Ecology*, 70, 503–507.

———————————
K. J. Anchukaitis, Lamont-Doherty Earth Observatory, Columbia University, 61 Route 9W, Palisades, NY 10946, USA. (kja@ldeo.columbia.edu)

M. N. Evans, Laboratory of Tree-Ring Research, University of Arizona, 105 West Stadium, Tucson, AZ 85721, USA.

D. P. Schrag, Department of Earth and Planetary Sciences, Harvard University, 20 Oxford St., Cambridge, MA 02138, USA.

N. T. Wheelwright, Department of Biology, Bowdoin College, 230B Druckenmiller Hall, Brunswick, ME 04011, USA.